ChemComm

COMMUNICATION

View Article Online
View Journal | View Issue

Cite this: *Chem. Commun.*, 2019, 55, 3745

Received 16th January 2019,
Accepted 25th February 2019

DOI: 10.1039/c9cc00384c

rsc.li/chemcomm

A magnetic covalent organic framework as an adsorbent and a new matrix for enrichment and rapid determination of PAHs and their derivatives in $PM_{2.5}$ by surface-assisted laser desorption/ionization-time of flight-mass spectrometry†

Yanhao Zhang,[a] Yuanyuan Song,[a] Jie Wu,[b] Ruijin Li,[ad] Di Hu,[a] Zian Lin *[b] and Zongwei Cai *[ac]

A magnetic covalent organic framework nanomaterial (Fe_3O_4@COFs) served as an adsorbent for enrichment and a new matrix for SALDI-TOF-MS analysis of PAHs and their derivatives in $PM_{2.5}$. The unique properties of Fe_3O_4@COFs in terms of high enrichment ability and matrix-free interference made it possible for sensitive analysis of low-concentration organic small-molecule pollutants in complex environmental samples.

$PM_{2.5}$, the particulate matter in air with a diameter less than 2.5 μm, is now a serious environmental problem all over the world, especially in some developing countries, like China.[1] $PM_{2.5}$ exposure could lead to different human diseases, such as lung injury and cardiac dysfunction,[2] and it has been proven that these adverse health effects have significant correlation with multiple $PM_{2.5}$ compositions like heavy metals and organic compounds.[3] Among the different $PM_{2.5}$ components, polycyclic aromatic hydrocarbons (PAHs) and their derivatives, nitro-PAHs (NPAHs) and hydroxy-PAHs (OHPAHs), have attracted people's attention. It is not only because they have high concentrations in $PM_{2.5}$, but also they have toxicities which could affect human health.[4] Therefore, the determination of PAHs and their derivatives in $PM_{2.5}$ is an important way to evaluate the possible health risks caused by $PM_{2.5}$ exposure. Conventional methods to determine PAHs, NPAHs and OHPAHs in $PM_{2.5}$ mostly involve gas chromatography-mass spectrometry (GC-MS) or liquid chromatography-mass spectrometry (LC-MS).[5] These methods can provide good selectivity and sensitivity and fulfil most analytical requirements, but they also have some limitations such as tedious sample preparations, complicated and time-consuming pre-treatment steps, long analysis times and the use of considerable amounts of expensive and toxic solvents. Therefore, the development of an alternative approach for rapid analysis of PAHs and their derivatives in $PM_{2.5}$ is highly desirable.

Matrix-assisted laser desorption/ionization-time of flight mass spectrometry (MALDI-TOF-MS) is a powerful analytical technique which was first reported in the 1980s.[6] It uses a suitable matrix, which is an energy absorbing compound, to convert laser energy to facilitate the desorption and ionization processes of non-volatile compounds. However, due to large interferences from conventional matrices such as α-cyano-4-hydroxycinnamic acid (CHCA) and 2,5-dihydroxybenzoic acid (DHB) in the low mass range (<500 Da), MALDI-TOF-MS could not be used to achieve the analysis of small molecules like PAHs. To solve this problem, "surface-assisted laser desorption/ionization-time of flight-mass spectrometry (SALDI-TOF-MS)" was developed with nanomaterials as matrices. In previous work, there have been many kinds of nanomaterials including carbon-based materials[7] and metal nanoparticles,[8] which have been explored as matrices in SALDI-TOF-MS for the detection of small molecules. Covalent organic frameworks (COFs) have attracted much attention in recent years because of their abundant interactions with other molecules and their tunable structures.[9] Multiple advantages have enabled COFs to be used in diverse fields like sample pre-treatment and catalysis.[10] But there has been limited previous work which has used COFs as matrices for the detection of small molecules using MALDI-TOF-MS.[11] In this work, due to the relatively low concentrations of PAHs and their derivatives in $PM_{2.5}$, a kind of novel magnetic COF (Fe_3O_4@COFs) was synthesized and, for the first time, used as an enrichment material and a SALDI matrix simultaneously. With Fe_3O_4@COFs as both the enrichment material and the matrix, SALDI-TOF-MS revealed intense signal and a clear matrix

[a] *State Key Laboratory of Environmental and Biological Analysis, Department of Chemistry, Hong Kong Baptist University, Hong Kong SAR, China. E-mail: zwcai@hkbu.edu.hk*

[b] *Ministry of Education Key Laboratory of Analytical Science for Food Safety and Biology, Fujian Provincial Key Laboratory of Analysis and Detection Technology for Food Safety, Department of Chemistry, Fuzhou University, Fuzhou, Fujian, P. R. China. E-mail: zianlini@fzu.edu.cn*

[c] *Guangzhou Key Laboratory of Environmental catalysis and Pollution Control, School of Environmental Science and Engineering, Institute of Environmental Health and Pollution Control, Guangdong University of Technology, Guangzhou, China*

[d] *Institute of Environmental Science, Shanxi University, Taiyuan, China*

† Electronic supplementary information (ESI) available. See DOI: 10.1039/c9cc00384c

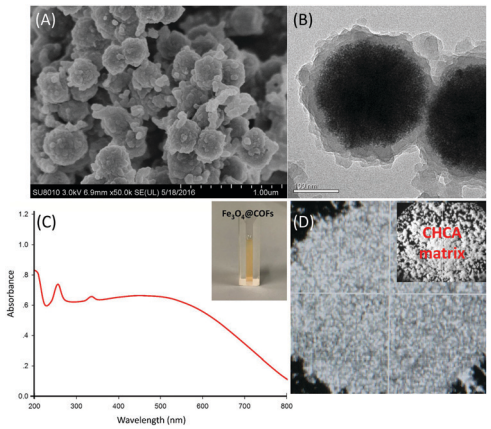

Fig. 1 (A) SEM and (B) TEM images of Fe_3O_4@COFs; (C) UV-visible spectrum of a 1 mg mL^{-1} Fe_3O_4@COFs suspension; (D) an optical image of 1 mg mL^{-1} Fe_3O_4@COFs.

background for analysis of $PM_{2.5}$-bound PAHs, NPAHs and OHPAHs with trace concentrations level.

The synthesis pathways of Fe_3O_4@COFs were described in our previous work.[12] Briefly, Fe_3O_4 nanoparticles were prepared by a solvothermal reaction. Then, the COF network was bonded to the Fe_3O_4 core by template-controlled precipitation polymerization of 1,3,5-tris(4-aminophenyl)benzene (TAPB) and terephthaldicarboxaldehyde (TPA) in dimethyl sulfoxide (DMSO) based on a Schiff-base reaction. The structure of Fe_3O_4@COFs was characterized by scanning electron microscopy (SEM) and transmission electron microscopy (TEM), as shown in Fig. 1A and B. The SEM image and the TEM image of Fe_3O_4@COFs revealed that the nanoparticles had good monodispersity and were well covered by COF shells with a thickness of ~25 nm. Other characterization data like an FT-IR spectrum is presented in Fig. S1 (ESI†).

To evaluate the feasibility of using Fe_3O_4@COFs as a SALDI matrix, the Fe_3O_4@COFs solution was tested by UV-visible spectroscopy. As shown in Fig. 1C, Fe_3O_4@COFs was well dispersed in water and the suspension had strong adsorption in the near UV region (~280 nm), which made it possible to absorb laser energy and transfer energy to analytes. At the same time, compared with a traditional matrix like CHCA, Fe_3O_4@COFs could achieve a homogeneous crystal layer with analytes (Fig. 1D), which is beneficial for SALDI analysis with low variability.

Based on our previous work,[12] Fe_3O_4@COFs showed relatively good performance in the enrichment of hydrophobic peptides. Due to the low concentration levels of the target compounds in $PM_{2.5}$, in order to improve the sensitivity of the method, in this work, Fe_3O_4@COFs was not only used as a SALDI matrix, but also as an adsorbent for enrichment. The enrichment behaviour was based on multiple interactions between Fe_3O_4@COFs and PAHs/NPAHs/OHPAHs. For example, hydrophobic interactions between Fe_3O_4@COFs and analytes are interactions which can enhance adsorption; π–π interactions between the benzene rings in the COF shells and PAHs/NPAHs/OHPAHs are propitious to the capture of analytes; hydrogen-bonding interactions between the COFs shells and the nitro/phenol-groups in NPAHs/OHPAHs are also favorable for adsorption. To enrich $PM_{2.5}$-bound PAHs, NPAHs and OHPAHs, a dried droplet method was selected for sample pre-treatment.[13] A total of 4 PAHs (biphenyl, acenaphthylene, phenanthrene, and pyrene), 4 NPAHs (1-nitronaphthalene, 3-nitrodibenzofuran, 9-nitroanthracene, and 7-nitrobenz[*a*]anthracene) and 4 OHPAHs (2-hydroxynaphthalene, 2-hydroxyphenanthrene, 4-hydroxybiphenyl, and 3-hydroxyfluorene) in $PM_{2.5}$ samples were analysed. The whole sample pre-treatment procedures are shown in Scheme S1 (ESI†). Because the enrichment performance can directly influence signal intensity of SALDI-TOF-MS, to obtain the best enrichment performance, different adsorption times (Fig. S2, ESI†) and enrichment dosages (Fig. S3, ESI†) were optimized. The trend of enrichment time was obvious, which was that after 20 min there was not a significant increase in the recovery. But for the added Fe_3O_4@COFs for enrichment, it also needed to be considered that Fe_3O_4@COFs would be directly used as the SALDI matrix after adsorption. Although the recovery was kept at a relatively stable level in different Fe_3O_4@COFs dosages (80–120%), the MS signal intensities had obvious differences when different amounts of Fe_3O_4@COFs were used as the SALDI matrix. Three model samples (pyrene, 7-nitrobenz[*a*]anthracene, and 2-hydroxyphenanthrene) were tested using SALDI-TOF-MS under different Fe_3O_4@COFs (matrix) dosages and 1 mg was the best (Fig. 2a–c). Instrumental laser energies were also optimized for better SALDI-TOF-MS intensities and 60% laser energy was the final choice (Fig. 2d–f). The laser energy could still be enhanced, but with the increase of laser energy, the signal of the background was also more intense. The detection of real samples may be influenced by this, so laser energy higher than 60% was not selected. To do a comparison, a matrix-first method was also tried for determination with Fe_3O_4@COFs as the matrix. The method only used Fe_3O_4@COFs as the matrix without the enrichment step to detect 100 ng pyrene, 7-nitrobenz[*a*]anthracene and 2-hydroxyphenanthrene using SALDI-TOF-MS (Fig. S4, ESI†). Fe_3O_4@COFs only as the matrix could provide good intensities for PAHs, NPAHs and OHPAHs. But after enrichment, with same amounts of target compounds, the MS signals were more intense. This was because after enrichment, higher ionization efficiency was obtained like the previous work.[13] The SALDI-TOF-MS spectra, recorded under optimized conditions, of 4 PAHs, 4 NPAHs and 4 OHPAHs are shown in Fig. S5 (ESI†). Based on chemical characteristics, both positive mode (PAHs) and negative mode (NPAHs and OHPAHs) were used for detection.[7b,14] PAHs had better signal to noise ratio (S/N) in positive mode than in negative mode. This was because the PAHs had relatively stable structures and did not have

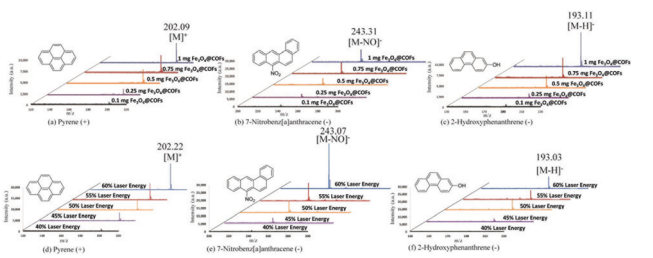

Fig. 2 Optimization of matrix dosage (a–c, laser energy: 50%) and laser energy (d–f, matrix dosage: 1 mg) with 100 ng of a single standard.

substituted groups such as those of the NPAHs and OHPAHs. The frameworks of Fe_3O_4@COFs with numerous aromatic rings could enhance the energy transfer to the PAHs through π electron stacking. This was the same as using graphene as a matrix to detect PAHs.[7b] In this work, the major ions of the PAHs that were produced were $[M]^+$. The characteristic $[M]^+$ ions of biphenyl, acenaphthylene, phenanthrene and pyrene had m/z values of 154.20, 152.19, 178.20 and 202.21 (Fig. S5, ESI†). According to the previous literature,[14] matrices with aromatic π-conjugated structures were beneficial for laser adsorption and energy transfer for the detection of NPAHs and OHPAHs in MALDI-TOF-MS, which means that Fe_3O_4@COFs may have a similar function. NPAHs and OHPAHs have substituted nitro (NO_2) groups and hydroxy (OH) groups, respectively. The NO_2 groups in NPAHs have strong electron affinities and they were easily ionized through negative-ion transfer reactions.[15] For OHPAHs, the benzene ring was a group with electron affinity when it was bounded to phenolic hydroxyl. The hydrogen group in the OH group was quite active and was easy to lose. So, the signals for the NPAHs and OHPAHs in MALDI-TOF-MS in negative mode were better than those in positive mode. In this work, the NPAHs produced $[M]^-$ and $[M–NO]^-$. The characteristic ions of 1-nitronaphthalene, 3-nitrodibenzofuran, 9-nitroanthracene and 7-nitrobenz[*a*]anthracene had m/z values of 173.11/143.15, 213.15/183.09, 223.16/193.20 and 243.16, respectively (Fig. S5, ESI†). The major peaks of the OHPAHs were $[M–H]^-$. The major ions had m/z values of 143.10, 193.14, 169.13, and 181.15 for 2-hydroxynaphthalene, 2-hydroxyphenanthrene, 4-hydroxybiphenyl and 3-hydroxyfluorene, respectively (Fig. S5, ESI†). The spectra of mix standards of PAHs, NPAHs and OHPAHs were also obtained (Fig. S6, ESI†). The blank of the pure Fe_3O_4@COFs, which was used as the matrix was also given in Fig. S6 (ESI†). As for the mixture of the standards, the response had a little decrease because of the increase in concentration of the compounds. Because of the limited resolution of SALDI-TOF-MS, the MS peaks of $[1\text{-nitronaphthalene} - NO]^-$/$[2\text{-hydroxynaphthalene} - H]^-$ and $[9\text{-nitronaphthalene} - NO]^-$/$[2\text{-hydroxyphenanthrene} - H]^-$ coincided (Fig. S6, ESI†). In order to do a comparison, backgrounds with the conventional matrix, CHCA, were obtained (Fig. S6e and f, ESI†). It was obvious that the intensities of the interference peaks (CHCA) in the small molecule regions were too high for CHCA to be used as the matrix.

To investigate the feasibility of using Fe_3O_4@COFs as an enrichment material and a SALDI matrix simultaneously, a real $PM_{2.5}$ sample was applied for analysis by this method. Detailed $PM_{2.5}$ sample collection is described in the ESI.† From Fig. 3a (positive mode) and Fig. 3b (negative mode), almost all target compounds in the $PM_{2.5}$ sample could be detected with Fe_3O_4@COFs as an enrichment material and a SALDI matrix. In positive mode, $[M]^+$ ions (PAHs) of biphenyl (a1), acenaphthylene (a2), phenanthrene (a3) and pyrene (a4) were observed (Fig. 3a). In negative mode, for NPAHs and OHPAHs, due to the overlap of molecule weights, the $[M–NO]^-$ ion of 1-nitronaphthalene and the $[M–H]^-$ ion of 2-hydroxynaphthalene (b1/c1), and the $[M–NO]^-$ ion of 9-nitroanthracene and the $[M–H]^-$ ion of 2-hydroxyphenanthrene (b3/c2) had the same MS peaks. In addition, in the NPAHs group, the $[M]^-$ ion of 1-nitronaphthalene (b1), and the $[M–NO]^-$ ions

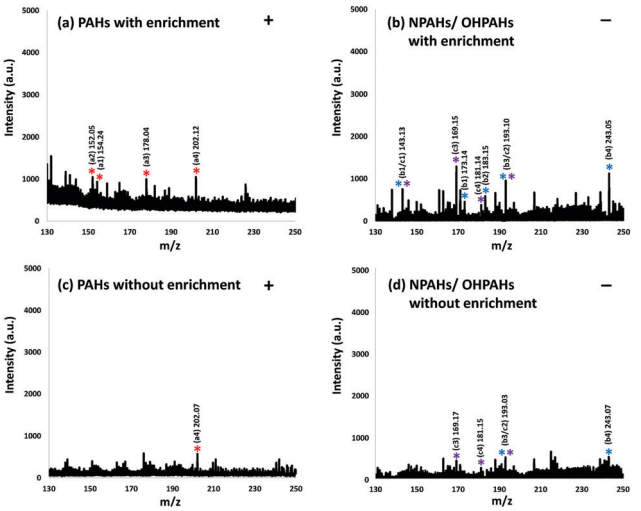

Fig. 3 Real sample SALDI-TOF-MS spectra with (a and b) and without (c and d) enrichment using Fe_3O_4@COFs ((a1) acenaphthylene; (a2) biphenyl; (a3) phenanthrene; (a4) pyrene; (b1) 1-nitronaphthalene; (b2) 3-nitrodibenzofuran; (b3) 9-nitroanthracene; (b4) 7-nitrobenz[*a*]anthracene; (c1) 2-hydroxynaphthalene; (c2) 2-hydroxyphenanthrene; (c3) 4-hydroxybiphenyl; (c4) 3-hydroxyfluorene).

of 3-nitrodibenzofuran (b2) and 7-nitrobenz[*a*]anthracene (b4) were observed. In the OHPAHs group, the $[M–H]^-$ ions of 4-hydroxybiphenyl (c3) and 3-hydroxyfluorene (c4) were detected. A parallel $PM_{2.5}$ sample was also analysed by SALDI-TOF-MS without enrichment for performance comparison. This parallel $PM_{2.5}$ sample was treated with ultrasonic extraction with 100 mL hexane/acetone (1 : 1, v/v). Then the extract was concentrated to 1 mL and used directly in SALDI-TOF-MS analysis only using Fe_3O_4@COFs as the matrix. Fig. 3c (positive mode) and Fig. 3d (negative mode) are MS spectra of the extract of the parallel $PM_{2.5}$ sample. Although the background signals of the MS spectra were more intense in Fig. 3a and b than in Fig. 3c and d, which was because Fe_3O_4@COFs did not have selectivity, so other containments also could be trapped, only pyrene in positive mode (Fig. 3c) and 4-hydroxybiphenyl, 3-hydroxyfluorene, 9-nitroanthracene/2-hydroxyphenanthrene, and 7-nitrobenz[*a*]anthracene in negative mode (Fig. 3d) could be detected without enrichment because of the low concentrations of the target compounds in $PM_{2.5}$. So, the enrichment function of Fe_3O_4@COFs played an important role in the determination of the PAHs and their derivatives in $PM_{2.5}$ by SALDI-TOF-MS.

Based on this method, a quantitative analysis was performed. Pyrene (PAH) and 7-nitrobenz[*a*]anthracene (NPAH) were selected as model compounds for positive and negative mode. Linear relationships (R^2 > 0.99) were found between the MS signal intensities and different amounts (0.1–100 ng) for pyrene (Fig. S7, ESI†) and 7-nitrobenz[*a*]anthracene (Fig. S8, ESI†). Fig. S9 (ESI†) shows the intensity reproducibilities of pyrene and 7-nitrobenz[*a*]anthracene with 10 continuous determinations using the developed method. The relative standard deviations (RSDs) were 6.3% for pyrene and 6.1% for 7-nitrobenz[*a*]anthracene and the values were acceptable for quantification analysis. The limit of detections (LODs), which were defined as 3 times the S/N,

of the model compounds were 0.08 ng (pyrene) and 0.01 ng (7-nitrobenz[*a*]anthracene). Their values were lower or at similar level compared with previous works.[14] The quantification results of the samples presented in Fig. 3a and b are listed in Table S1 (ESI†). In order to confirm the results from SALDI-TOF-MS, the samples were also tested by GC-MS, based on our previous developed method[16] and the results are listed in Table S1 (ESI†). In Table S1 (ESI†), the quantification results of pyrene and 7-nitrobenz[*a*]anthracene are in good accordance with those obtained by GC-MS, which means that the results from SALDI-TOF-MS are credible.

In conclusion, we firstly developed the Fe_3O_4@COFs as an adsorbent and matrix for the determination of PAHs, NPAHs and OHPAHs in $PM_{2.5}$ by SALDI-TOF-MS in different modes. Compared to the conventional method, this method was more rapid without complicated sample preparation and long instrumental running time for the determination of PAHs and their derivatives in $PM_{2.5}$. Based on our work, it was found that Fe_3O_4@COFs had a relatively clear background in the SALDI-TOF-MS small molecule region when it was used as a matrix. At the same time, its specific structure made it provide high sensitivity as a matrix and give an enrichment function for some small molecule organic pollutants. Therefore, the Fe_3O_4@COFs had good potential for rapid determination of trace and ultra-trace level organic pollutants in complex environmental matrices as an adsorbent and a matrix simultaneously.

This study was supported by the National Natural Science Foundation of China (91543202 and 21675025), the Collaborative Research Fund (C2014-14E) from the Research Grants Council of Hong Kong and National Key research and development program-cooperation on scientific and technological innovation in Hong Kong, Macau and Taiwan (2017YFE0191000).

Conflicts of interest

There are no conflicts to declare.

Notes and references

1 Y. L. Zhang and F. Cao, *Sci. Rep.*, 2015, **5**, 14884.
2 (*a*) M. Gualtieri, J. Øvrevik, S. Mollerup, N. Asare, E. Longhin, H. J. Dahlman, M. Camatini and J. A. Holme, *Mutat. Res., Fundam. Mol. Mech. Mutagen.*, 2011, **713**, 18–31; (*b*) Z. Dagher, G. Garcon, S. Billet, P. Gosset, F. Ledoux, D. Courcot, A. Aboukais and P. Shirali, *Toxicology*, 2006, **225**, 12–24; (*c*) H. Wang, X. Shen, G. Tian, X. Shi, W. Huang, Y. Wu, L. Sun, C. Peng, S. Liu, Y. Huang, X. Chen, F. Zhang, Y. Chen, W. Ding and Z. Lu, *Free Radical Biol. Med.*, 2018, **121**, 202–214.
3 (*a*) W. J. Deng, P. K. K. Louie, W. K. Liu, X. H. Bi, J. M. Fu and M. H. Wong, *Atmos. Environ.*, 2006, **40**, 6945–6955; (*b*) R. B. Schlesinger, *Inhalation Toxicol.*, 2007, **19**, 811–832.
4 (*a*) R. Li, L. Zhao, L. Zhang, M. Chen, C. Dong and Z. Cai, *Environ. Toxicol. Pharmacol.*, 2017, **54**, 14–20; (*b*) K. B. Okona-Mensah, J. Battershill, A. Boobis and R. Fielder, *Food Chem. Toxicol.*, 2005, **43**, 1103–1116; (*c*) L. R. Wang, Y. Wang, J. W. Chen and L. H. Guo, *Toxicology*, 2009, **262**, 250–257.
5 (*a*) M. Niederer, *Environ. Sci. Pollut. Res. Int.*, 1998, **5**, 209–216; (*b*) M. R. Mannino and S. Orecchio, *Atmos. Environ.*, 2008, **42**, 1801–1817; (*c*) R. Avagyan, R. Nyström, C. Boman and R. Westerholm, *Anal. Bioanal. Chem.*, 2015, **407**, 4523–4534; (*d*) F. Fujiwara, M. Guiñez, S. Cerutti and P. Smichowski, *Microchem. J.*, 2014, **116**, 118–124.
6 M. Karas, D. Bachmann, U. Bahr and F. Hillenkamp, *Int. J. Mass Spectrom. Ion Processes*, 1987, **78**, 53–68.
7 (*a*) M. Lu, Y. Lai, G. Chen and Z. Cai, *Anal. Chem.*, 2011, **83**, 3161–3169; (*b*) J. Zhang, X. Dong, J. Cheng, J. Li and Y. Wang, *J. Am. Soc. Mass Spectrom*, 2011, **22**, 1294–1298.
8 (*a*) Y. Gholipour, S. L. Giudicessi, H. Nonami and R. Erra-Balsells, *Anal. Chem.*, 2010, **82**, 5518–5526; (*b*) Y. F. Huang and H. T. Chang, *Anal. Chem.*, 2006, **78**, 1485–1493.
9 N. W. Ockwig, A. P. Co, M. O. Keeffe, A. J. Matzger and O. M. Yaghi, *Science*, 2005, **310**, 1166–1171.
10 (*a*) H. Xu, X. Chen, J. Gao, J. Lin, M. Addicoat, S. Irle and D. Jiang, *Chem. Commun.*, 2014, **50**, 1292–1294; (*b*) W. Zhang, F. Liang, C. Li, L. G. Qiu, Y. P. Yuan, F. M. Peng, X. Jiang, A. J. Xie, Y. H. Shen and J. F. Zhu, *J. Hazard. Mater.*, 2011, **186**, 984–990; (*c*) W. Zhang, Y. Zhang, Q. Jiang, W. Zhao, A. Yu, H. Chang, X. Lu, F. Xie, B. Ye and S. Zhang, *Anal. Chem.*, 2016, **88**, 10523–10532.
11 D. Feng and Y. Xia, *Anal. Chim. Acta*, 2018, **1014**, 58–63.
12 G. Lin, C. Gao, Q. Zheng, Z. Lei, H. Geng, Z. Lin, H. Yang and Z. Cai, *Chem. Commun.*, 2017, **53**, 3649–3652.
13 Z. Lin, W. Bian, J. N. Zheng and Z. W. Cai, *Chem. Commun.*, 2015, **51**, 8785–8788.
14 (*a*) W. Lu, Y. Li, R. Li, S. Shuang, C. Dong and Z. Cai, *ACS Appl. Mater. Interfaces*, 2016, **8**, 12976–12984; (*b*) J. Zhang, L. Zhang, R. Li, D. Hu, N. Ma, S. Shuang, Z. W. Cai and C. Dong, *Analyst*, 2015, **140**, 1711–1716.
15 B. M. Hughes, C. Lifshitz and T. O. Tiernan, *J. Chem. Phys.*, 1973, **59**, 3162–3181.
16 (*a*) Y. Zhang, Y. Chen, R. Li, W. Chen, Y. Song, D. Hu and Z. Cai, *Talanta*, 2019, **195**, 757–763; (*b*) Y. Zhang, R. Li, J. Fang, C. Wang and Z. Cai, *Chemosphere*, 2018, **198**, 303–310; (*c*) R. J. Li, X. J. Kou, H. Geng, C. Dong and Z. W. Cai, *Chin. Chem. Lett.*, 2014, **25**, 663–666.

